Airborne Electromagnetic Survey over the Touro Copper VMS World Class Deposit (NW Spain): Geological and Geophysical Correlation

Pablo Núñez [1] , Tony Watts [2], Agustín Martin-Izard [3],*, Daniel Arias [3], Álvaro Rubio [3], Fernando Cortés [4] and Fernando Díaz-Riopa [4]

[1] Cobre San Rafael, O Pino, 15823 A Coruña, Spain
[2] Consulting Geophysicist, Suite 807, 650 Queens Qway West, Toronto, ON M5V 3N2, Canada
[3] Department of Geology, University of Oviedo, 33005 Oviedo, Spain
[4] Atalaya Mining, La Dehesa, Minas de Riotinto, 21660 Huelva, Spain
* Correspondence: amizard@uniovi.es

Abstract: Electromagnetic (EM) methods belong to the main geophysical techniques used in the mineral exploration of massive sulphides. For selecting EM anomalies as possible massive sulphide targets, it is important to combine the geophysical results with other geological and/or geochemical techniques. In 2015, Atalaya Mining started a new mineral exploration project in the Touro Cu deposit, combining geological, geochemical (ore over 0.2% Cu), and geophysical techniques. The geophysical survey consisted of helicopter-borne EM using the versatile time-domain electromagnetic (VTEM™) max system operated by Geotech Ltd. with full-waveform processing. In total, 509 line-km of geophysical data were acquired during the survey that was completed in 2018. The results showed the massive sulphide Touro ore to be typically of the order of 0.25 ohm·m (4S/m conductivity) and host rock in the range of 1000–30,000 ohm·m, measured directly on the drill core. This modelling agreed well with the sub-horizontal dips observed for the known Touro ore bodies. The conductance modelled by the plate estimation of the VTEM data were also in good agreement with those provided by Geotech Ltd. and the resistivity/conductivity measurements we made on the massive sulphide samples from several Touro ore bodies. The combination of flat dips, good conductance, shallow depth, and, lastly, lack of conductive overburden or noneconomic conductive stratigraphy, i.e., graphitic shales and sulphide iron formation make the Touro project an ideal target for airborne electromagnetic prospecting. This paper presents the excellent correlation observed between the EM airborne anomalies and the massive sulphide blocks of the Touro copper deposit. Favourable factors contributing to the success of the survey were the high contrast in resistivity/conductivity between the massive sulphide Touro ore and the amphibolite host rock and minimal interference from "nuisance" conductors, such as graphitic shales.

Keywords: airborne electromagnetic survey; copper VMS deposit; Touro; NW Spain; new exploration targets

1. Introduction

The main purpose of mineral exploration is to discover new ore deposits. For selecting the best targets for drilling, it is necessary to have a good knowledge of the geological, geochemical, and geophysical features of the prospective area [1,2]. Geophysical methods have played an important role in the discovery of sulphide deposits [3–10], and the EM methods belong to the main geophysical techniques used in the mineral exploration of massive sulphides [11,12]. With airborne or surface EM, it is possible to identify conductive massive sulphide deposits as a response between the different conductivity of the ore (over 0.2% Cu) and the host rock resistivity. The problem is that different geological lithologies

can cause similar anomalies. Materials such as graphite and clay can produce EM anomalies similar to those of massive sulphides, as reflected by reported conductivity data [13,14].

For selecting possible EM anomalies as massive sulphide targets, it is important to combine the geophysical results with other geological and/or geochemical techniques. The joint interpretation of geological, geochemical, and geophysical data is an important procedure in the identification of mineral exploration targets [15,16].

The Touro copper ore deposit was discovered by Rio Tinto Patiño, S.A., in the 1970s, with resources of 32 Mt, with 0.57% Cu [17,18]. Mining of the deposit commenced in 1973 at the rate of 1.5 Mt per year until 1986, when the mine was closed due to low copper prices. In 2015, Atalaya Mining started a new mineral exploration project in Touro, combining geological, geochemical, and geophysical techniques, including 424 drill cores. With these data, Atalaya Mining defined a new ore deposit with resources of 103 Mt with 0.41% Cu [19].

In 2017, Atalaya carried out an airborne EM survey using the Geotech Ltd. VTEM helicopter system. This paper presents the excellent correlation observed between the EM airborne anomalies and the massive sulphide blocks of the Touro copper deposit. A favourable lithology and a structure hosting massive sulphides were the main keys for this good correlation.

2. Geological Setting

The Touro copper ore deposit is located in the NW of the Iberian Variscan Belt (Figure 1A). The copper ore bodies are hosted in the Ordenes complex, one of the four allochthonous complexes of the Galicia-Trás-Os-Montes Zone [20,21] (Figure 1B). The VTEM survey area is located on the Fornás Unit in the south-western part of the Órdenes Complex (Figure 1B).

The Touro copper ore deposit is hosted by a thick sequence of turbidites (pelites and greywackes), with mafic volcanic rocks interbedded, deposited during the Ordovician in a back-arc basin [22]. These rocks are located in the upper part of the Ordenes Complex and show a high-pressure and high-temperature (HP-HT) metamorphism involving the transformation of the original siliciclastic lithology in paragneisses and amphibolites [23,24].

According to our geological map and cross-sections, the host rocks of the Touro copper ore deposit are folded by the Arinteiro antiform formed during the last stage of the Variscan orogenesis. Mineralised rocks in the antiform are predominantly garnet amphibolites interbedded with paragneisses exhibiting lenticular morphology (Figure 2). The Touro copper deposit complex is composed of seven different bodies named, Arinteiro, Vieiro, Monteminas, Arca, Bama, Brandelos, and Fuente Rosas (Figure 2). Each of these bodies is an individual deposit with its own feeder zone [22]. The copper grade is higher in the feeder zone and decreases in all directions. The favourable ore-hosting stratigraphy has a strike length of 6 km and is open to the east and west, with several outcrops of sulphides hosted by Ca-poor amphibolites.

The ore body structure is flat and tabular. In the east limb of the Arinteriro antiform, there are two ore blocks, Vieiro and Arinteiro, with the bedding dipping between 5° and 35° to the east. In the west limb, there are four ore blocks, Arca, Bama, Brandelo, and Fuente Rosas, with the bedding from 10° to 35° dipping west. In the hinge zone, there is the Monteminas ore body, which is dipping 5° to 25° east and west.

The mineralisation is present as massive sulphides and stringers, mainly in the amphibolite (90%) and locally in paragneisses (10%). The metallic minerals consist of pyrrhotite, chalcopyrite, sphalerite, and minor pyrite. The sulphides are enclosed in a Ca-poor amphibolite [22].

The genesis of the Touro copper deposit can be classified as a volcanic massive sulphide (VMS) of the mafic-siliciclastic type (old Besshi type) [22].
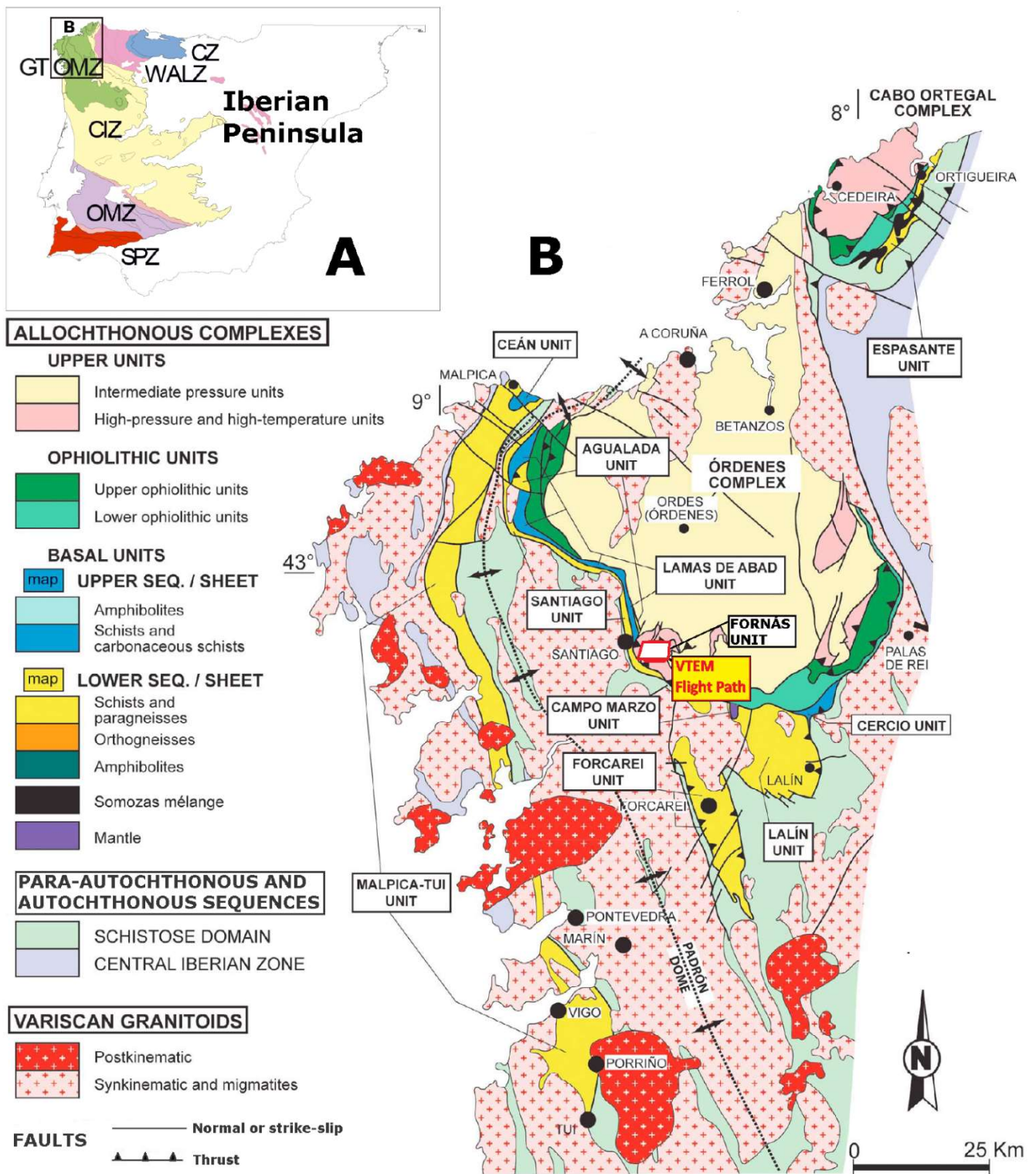
Figure 1. (**A**) Geological sketch of the Iberian Variscan Massif. CZ: Cantabrian Zone, WALZ: West Asturian Leonese Zone, CIZ: Central Iberian Zone, OMZ: Ossa Morena Zone, and SPZ: South Portuguese Zone [25,26]. (**B**) Geological map of the NW Iberian Variscan Massif showing the location of the Ordenes and Cabo Ortegal allochthonous complexes, as well as units of Galicia-Trás-Os-Montes Zone [26] and the Central Iberian Zone [22].
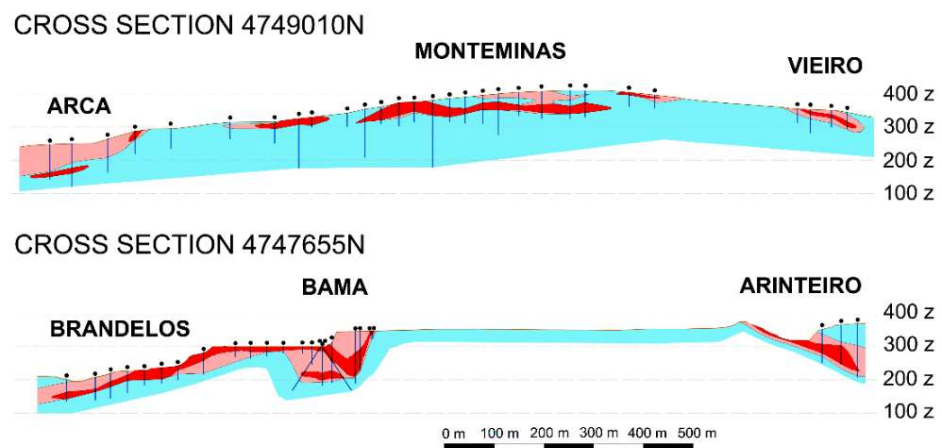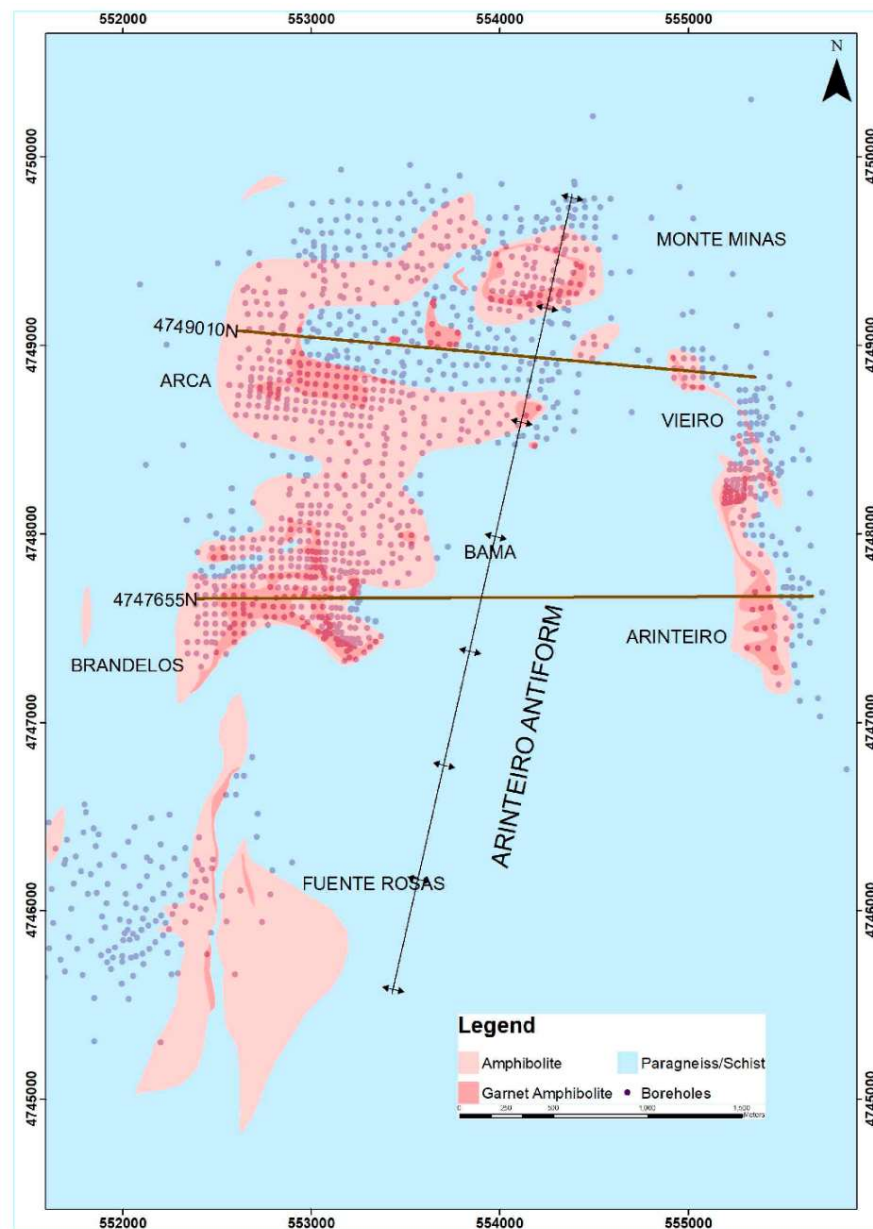
Figure 2. Geological map and cross-sections with borehole locations of the Touro copper deposit. All map co-ordinates are in UTM, and Z is in meters.

3. VTEM Methodology

A detailed geological map and cross-section was initially completed. Moreover, the ore bodies were defined by a copper content over 0.2%. Using this geological map, the EM helicopter-borne geophysical research was planned and performed by Geotech Ltd. (Ontario, Canada). The geophysical surveys consisted of helicopter-borne EM using the versatile time-domain electromagnetic (VTEM™) Max system with full-waveform processing [27] and an aeromagnetic total field using a caesium magnetometer. The measurements consisted of the vertical (Z) and in-line horizontal (X) dB/dt components of the EM fields using induction coils. In total, 509 line-km of geophysical data were acquired during the survey that was completed in 2018, with a line spacing of 100 m and flight direction N90° E/N270° E (Figure 3).
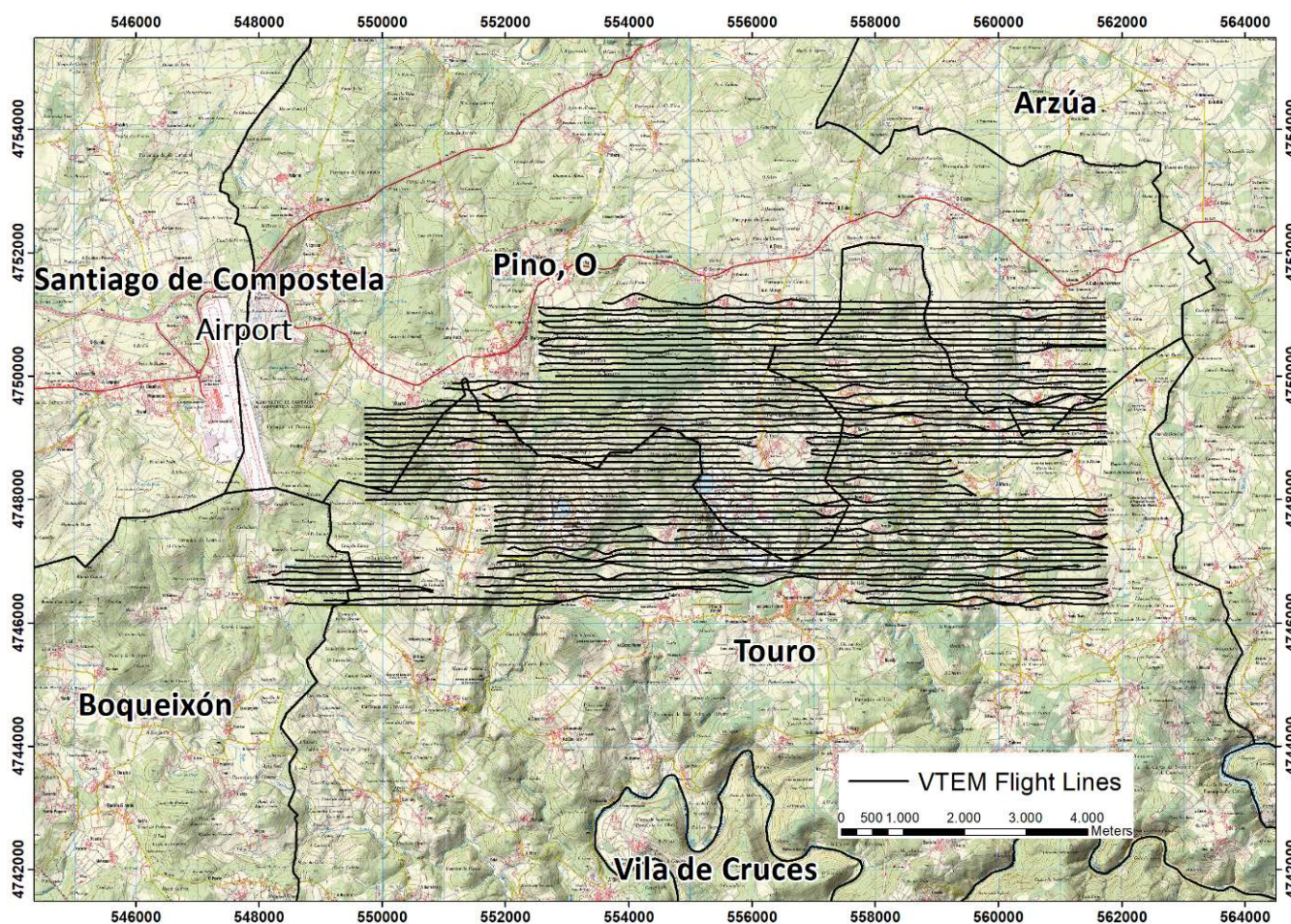

Figure 3. VTEM flight path on a topographic map of the area.

During the survey, the helicopter maintained a mean altitude of 108 m above the ground, with an average survey speed of 80 km/h. This allowed for an actual average transmitter–receiver loop terrain clearance of 60 m and a magnetic sensor clearance of 98 m.

The electromagnetic system used for the data acquisition was a Geotech Time Domain EM (VTEM™max, Serial number 36), which uses the streamed half-cycle recording of transmitter and receiver waveforms. The equipment uses 43 time gates of measurement in the range from 0.021 to 8.083 msec. The Geotech data acquisition system recorded the digital data on an internal compact flash card. Data compilation and processing were carried out using the Geosoft OASIS Montaj application and Geotech Ltd. programs.

The processing of the magnetic data involved the correction for diurnal variations by using the digitally recorded ground magnetic values. The aeromagnetic data were corrected for diurnal variations by subtracting the observed magnetic base station deviations.

4. Comparison of Measured VTEM Data with Geological Sections

Preliminary processing was carried out on a daily basis during the acquisition phase to avoid mistakes and for data quality assurance. The results are presented as stacked profiles of EM voltages for the times gates, in linear–logarithmic scale for the B-field component, and dB/dt responses in the Z and X components. The B-field Z component is presented by the time channel recorded at 1.161 milliseconds after the termination of the impulse.

From the 43 dB/dt profiles' Z component, time gates 0.210–7.036, three maps were designed of the VTEM EM anomalies for channels SFz20 (time gate 0.220 ms), SFz25 (time gate 0.440 ms), and SFz30 (time gate 0.880 ms). The preliminary correlation analysis between the local geology of the Touro ore body and the VTEM anomaly maps concluded that better resolution was obtained in the SFz25 map. The conductive anomalies shown in the map can be interpreted as structural conductors, lithological conductors, and anthropic conductors. The anomalous zones had dB/dt time constants ranging from about 0.2 to 5.36 ms. The apparent resistivity of the anomalous zones was estimated to be less than 150 Ohm·m. According to the apparent resistivity depth images over all lines, the estimated depth of the anomalous zones was approximately from the near surface to 120 m. The aeromagnetic data are shown in a total magnetic intensity (TMI) reduced to pole (RTP) colour map.

As mentioned in the introduction, the success of an airborne electromagnetic survey in the exploration for massive sulphide-related base metals is highly correlated with the resistivity contrast between the target mineralization and the enclosing host rock [11,28]. In this regard, extensive resistivity measurements were carried out on drill cores from most of the known Touro ore bodies. The results showed the massive sulphide Touro ore to be typically of the order of 0.25 ohm·m (4S/m conductivity) and host rock in the range of 1000–30,000 ohm·m. In the course of this testing, the only evidence of graphite, which is a source that could give rise to a false positive EM response, was from the Fuente Rosas ore body. At Touro, the graphite-bearing samples rarely fell below a resistivity of 100 ohm·m, implying that it was safe to assume that, in this case, graphite would not interfere to any significant degree in the detection of economic mineralisation on the Touro project. In other projects, the presence of clay or graphite can produce EM anomalies that interfere with the definition of VMS targets [13,14].

To demonstrate the correlation between the EM anomalies of the VTEM profiles and a typical Touro ore zone (over 0.2% Cu), the AR-5 geology cross-section across the Monteminas ore body was plotted underneath the profiles of the VTEM SFz EM (Figure 4). For the location of Section AR-5, see Figure 5. The ~50 m thick massive sulphide intercepts centred on 554,300 correlated with the peak VTEM response on L1150 and showed conductance from 47 to 70 Siemens in the Monteminas North Block. In the geological section, one can observe the Monte Minas North block in the hinge and east limb of the Arinteiro antiform, with the bedding dipping from 10° to 25° east, and, in the west limb, the Arca North block dips 30° west.

The results of the 2018 VTEM survey were refined using the EM anomalies with conductance > 20 Siemens (Figure 5). The best resolution was obtained in the EM profiles SFz25, Fraser-filtered dB/dt Z component channel 25 (time gate 0.440 ms) (Figure 6). For every survey line, we delineated the anomaly colour picks with >20 Siemens. All the Touro ore bodies with grade > 0.2%Cu presented an EM anomaly with pick values up to 88 Siemens (L1374 in the Arinteiro ore body). Fifteen new anomalies were delineated, T1 to T15, with Siemens pick values > 20. The maximum value was obtained in the F14 target, with a pick value of 298 Siemens (L1241) (Figures 5 and 6).

There were also EM cultural anomalies not delineated, i.e., the anomaly located to the SE of the Arinteiro–Veiro ore block in Figure 6, related to the tailing pond of the Riotinto Patiño old mine.

The aeromagnetic map is shown in Figure 7 as total magnetic intensity (TMI) reduced to pole (RTP). In this map, we delineated the existing ore blocks of the Touro VMS (blue outlines) and the EM anomalies of the new targets (black outlines). In general, the magnetic

anomalies were less well-defined than the EM anomalies, and the relationship with the known ore bodies was also less clear. The same conclusions were obtained with the EM anomalies of the new targets. The intense aeromagnetic anomaly, located to the SE of the Arinteiro–Veiro block, is related to the tailing dump of the old Riotinto Patiño mine. In the waste material, there is between 10% and 35% of pyrrhotite.
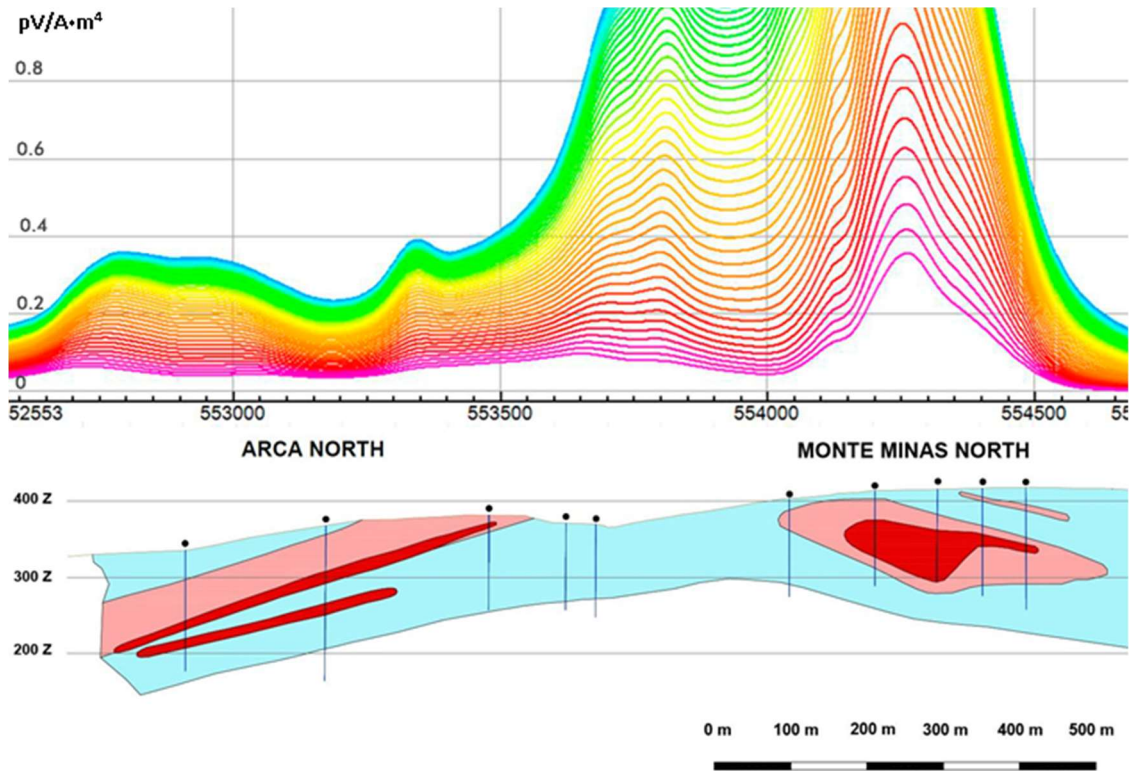

Figure 4. VTEM SfZ transients on the flight line L1150 plotted above the AR-5 geology section (legend in Figure 2).
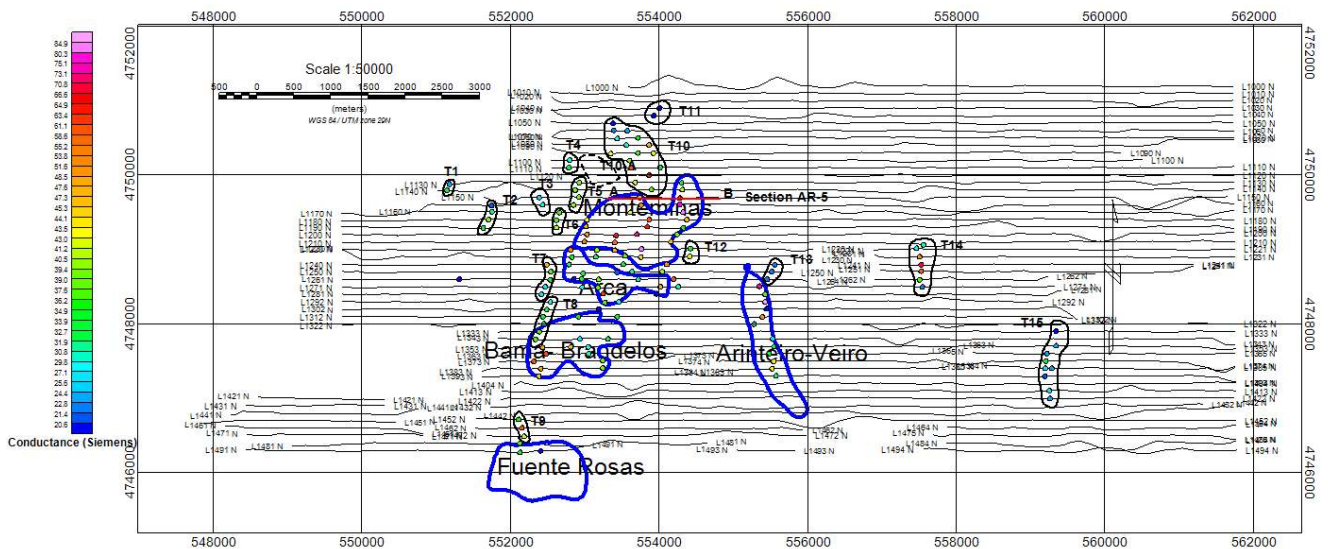

Figure 5. VTEM anomaly picks with >20 Siemens conductance with selected targets outside of known ore zone, labelled T1 to T15. Black outlines are the 15 new anomalies detected. Blue lines are the existing ore blocks of the Touro VMS deposit.
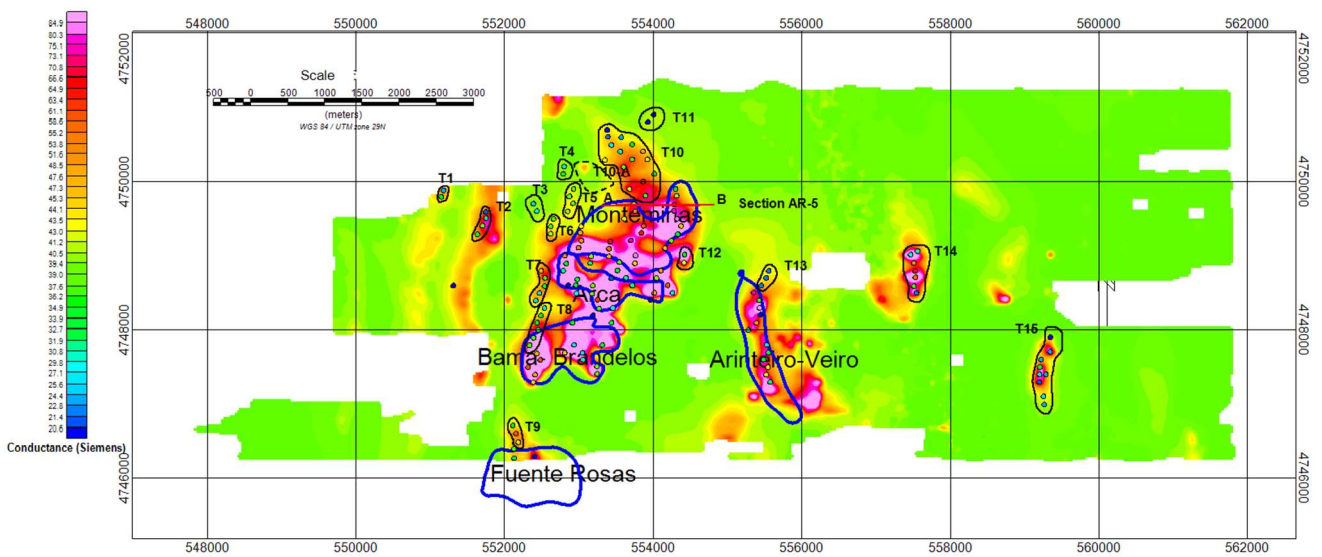
Figure 6. VTEM EM channel SFz25 (coloured background), known ore bodies (blue outlines). VTEM anomaly pick coloured symbols, with values > 20 Siemens, permitting the definition of additional areas of interest identified as targets T1 to T15 (black outlines). The cultural anomalies were not delineated.
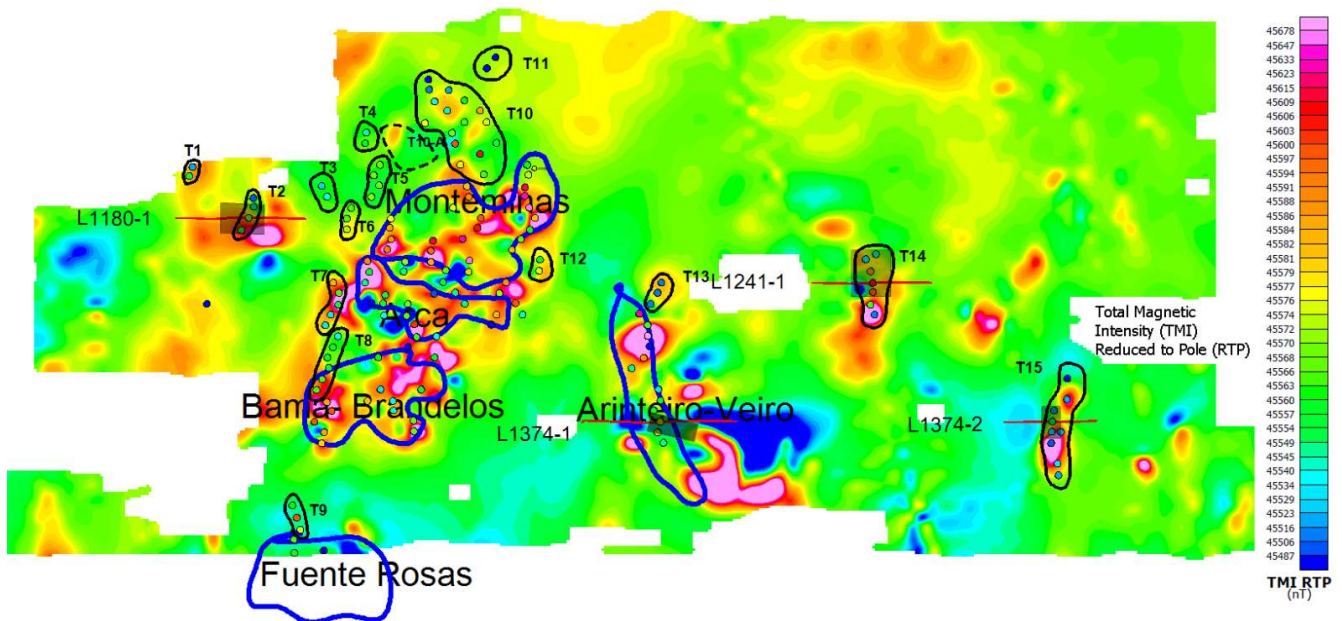

Figure 7. Total field magnetic colour image, known ore bodies (blue outlines), and colour dots with values > 20 Siemens. VTEM sections modelled in Maxwell ElectroMagnetic Imaging Technology (red horizontal line) with plates in Figures 8–11.
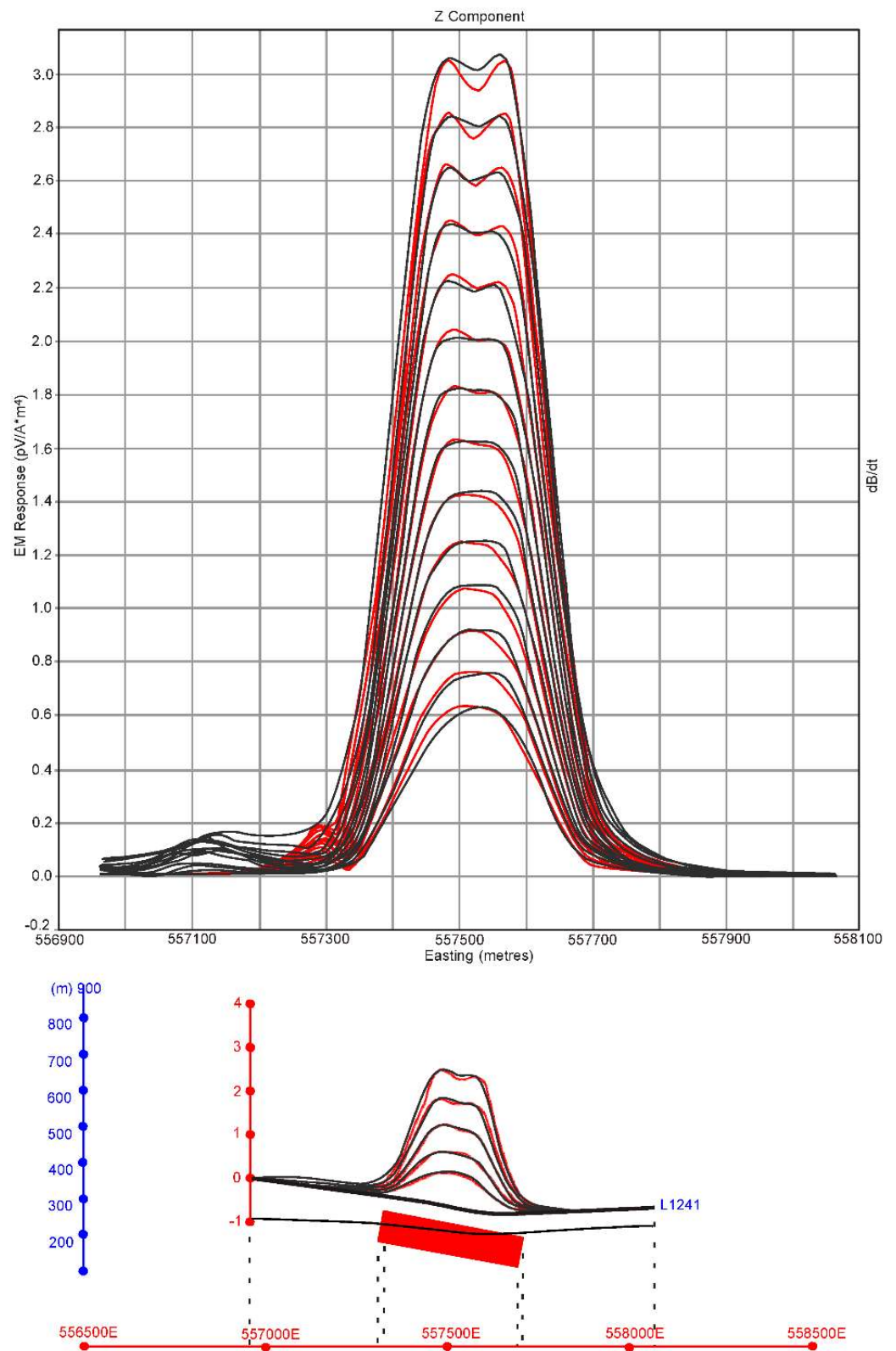
Figure 8. Maxwell thick plate modelling of the T-14 Target, facing north. The black lines are the field data of the Z component of the VTEM flight line L1241-1 and the red lines indicate the signals from the modelled plate. The top of the modelled conductor is close to surface and dips 10° east, with a conductance of 320S. It has a strike length of 370 m. In Figures 8–11, m means meters above sea level.
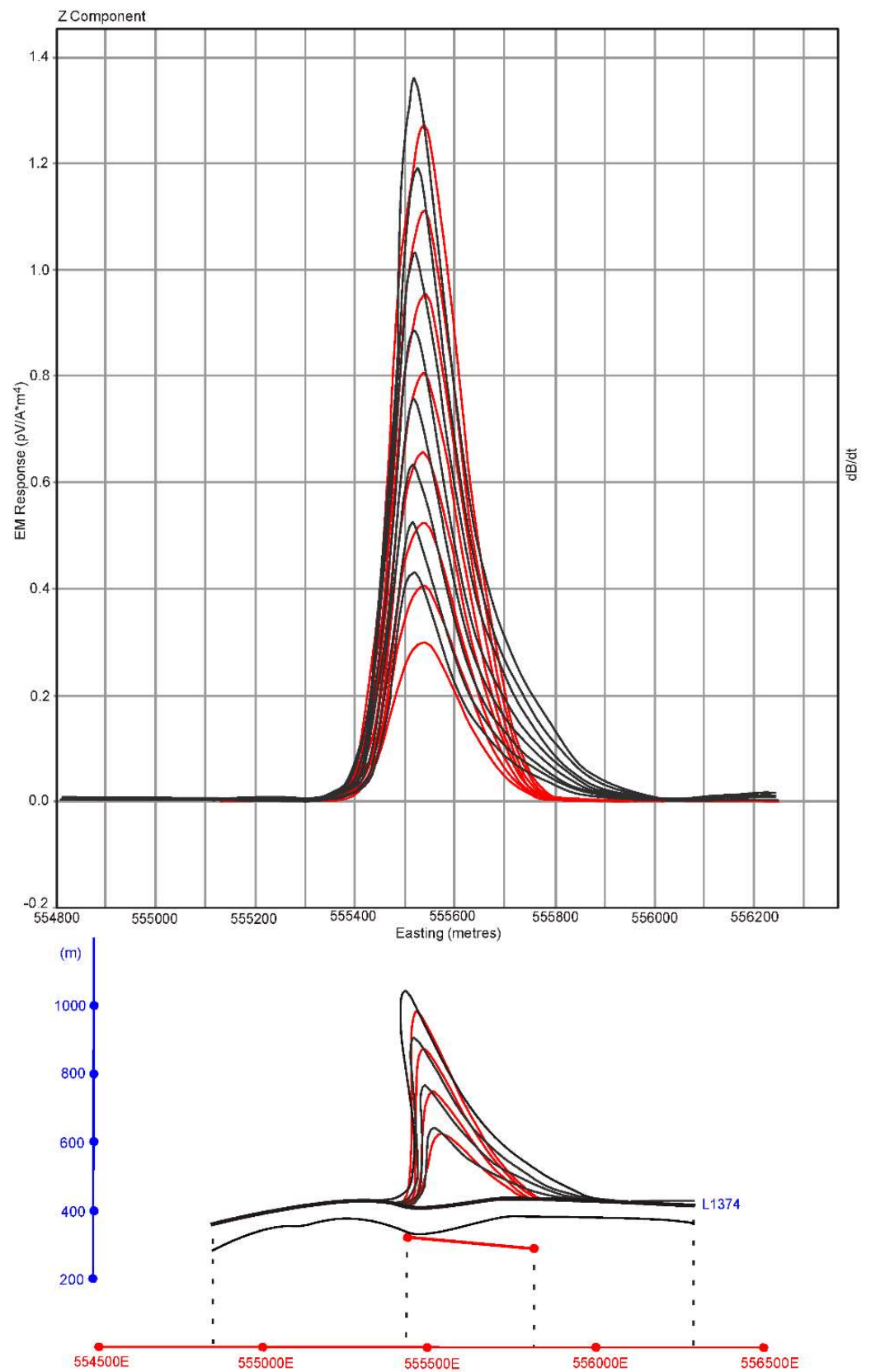
Figure 9. Maxwell thin plate modelling of the L1374-1 Arinteiro zone, facing north. The black lines are the field data of the Z component of the VTEM flight line L1374-1 and the red lines indicate the signals from the modelled plate. The top of the modelled conductor is close to surface and dips 5° east, with a conductance of 104S. It has a strike length of 375 m.
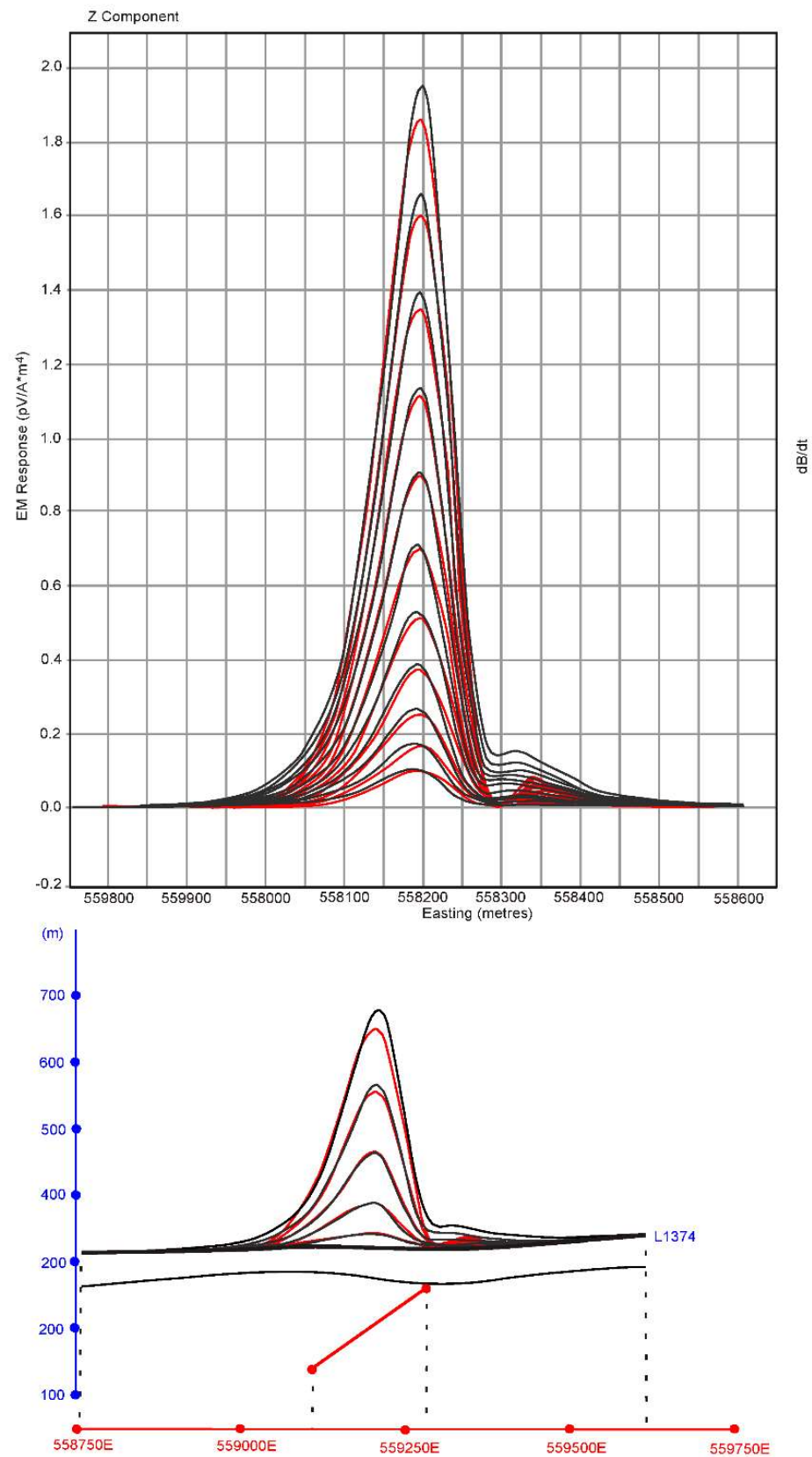
Figure 10. Maxwell thin plate modelling of the L1374-2, T-15 target, facing north. The black lines are the field data of the Z component of the VTEM flight line L1374-2 and the red lines indicate the signals from the modelled plate. The top of the modelled conductor is close to surface and dips 35° west, with a conductance of 90S. It has a strike length of 425 m.
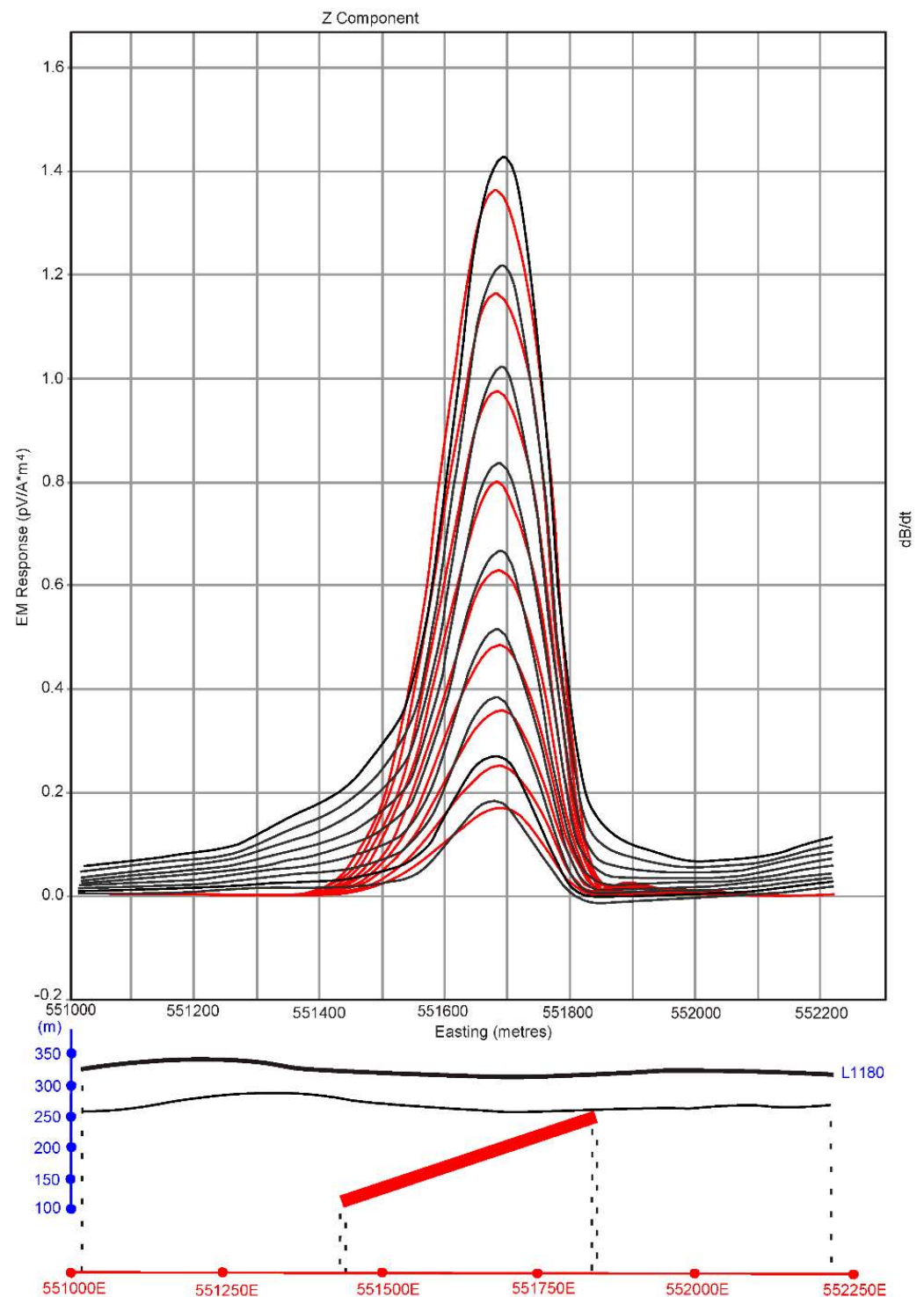
Figure 11. Maxwell thick plate modelling of the L1180, T-2 target, facing north. The black lines are the field data of the Z component of the VTEM flight line L1180 and the red lines indicate the signals from the modelled plate. The top of the modelled conductor is close to surface and dips 20° west, with a conductance 81S.

5. Modelling

Plate modelling of E–W trending anomalies was carried out on new targets judged to be of the highest priority, i.e., T2, T14, and T15, as well as the profile across the centre of the Arinteiro deposit (L1374-1 Section). They were constructed facing north. The selection of specific anomalies in the Touro area was made based on geological and structural

information available in the zone of the surveyed area, as well as the simplicity of the VTEM responses.

The VTEM sections were modelled in 3D Maxwell Electro Magnetic Imaging Technology developed by EMIT (Perth, Australia). The starting resistivity values for the background and the anomaly model were chosen from petrophysical studies. Plate dimensions and orientations were obtained from the Touro geological model [22]. The most important of these parameters are dip direction and strike length, together with information about the line spacing for the survey. Maxwell plate modelling was refined in several approaches.

We have used this modelling of plate targets because the results were clearer and present good correlation with the Touro geological model, compared to the inversion modelling. The inversion modelling showed negative results and the plate models had no correlation with the geological Touro ore blocks. This is because the real conductivity of the earth is a continuous function. Thus, the electromagnetic inverse problem does not have a unique solution and multiple models can be obtained. In our case, there was a high degree of model data misfit, with an important error in the inversion Maxwell plate modelling.

The four VTEM anomalies selected have been modelled using Maxwell thin plate, in sectors 1 and 2, of line L1374 and Maxwell thick plate in lines L1241-1 and L1180, located in Figure 7. Maxwell's plate algorithm assumes that the conductive plate is in a very resistive host. To obtain this approximation, we used data from the mid-time and late-time channels, channels 20 to 30 in our case, leaving just the conductive response of the targets for modelling. From the modelling, it is possible to obtain size, shape, depth, and dip angle of one conductor and its VTEM response in X and Z components. According to the geological model of the Touro ore body (22), the Maxwell plate modelling was conducted in the Z component, because the ore blocks are essentially tabular, with reduced thickness in comparison with the other two dimensions.

When the conductive plate is horizontal, the VTEM response in the Z component is a single peak just above the target. For a vertical conductive plate, the Z component VTEM response is a double peak located on the top of the conductor for thin plate and, for thick plate, there is a single peak with a wide bottom. If the conductive plate is dipping more than about 40°, the Z component of the EM response is a major peak and a minor peak.

The results of the thick plate modelling of L1241-1, target T-14, is shown in Figure 8. The black lines are the field data of the Z component of the VTEM flight line L1241 and the red lines indicate the signals from the modelled plate. The top of the conductor is close to the surface. It has a strike length of 370 m, a conductance of 320 Siemens, and 10° dipping to the east.

Figure 9 shows the Maxwell thin plate modelling of line L1374-1 on the Arinteiro ore block. The top of the conductor is close to the surface. It has a strike length of 375 m, a conductance of 104 Siemens, and 5° dipping to the east.

The Maxwell thin plate modelling of line L-1374-2, target T-15, is shown in Figure 10. The top of the conductor is close to the surface. It has a strike length of 425 m, a conductance of 90 Siemens, and 35° dipping to the west.

The last model made was the Maxwell thick plate modelling of line L1180, target T-2 (Figure 11). The top of the conductor is close to the surface. It has a strike length of 300 m, a conductance of 81 Siemens, and 20° dipping to the west.

All four single-plate models reasonably fit with the field data. The overall error for the Z component was regarded as low, as it was less than 5%.

The dip directions of three of the four plates were consistent with the location at the Arinteiro antiform. L1241 and L1374 are located on the eastern flank of the antiform and dip to the east. L1180 is located on the western flank of the antiform and dips to the west.

6. Conclusions

Plate modelling of VTEM airborne data confirmed the geometry and conductivity of ore bodies already known from drilling. In addition, large-scale VTEM flights detected previously unknown ore bodies. The dip directions of three of the four plates shown were

consistent with the location of the Arinteiro antiform. Lines L1241 and L1374 are located on the eastern flank of the antiform and dip to the east; L1180 is located on the western flank of the antiform and dips to the west. Modelling of the easternmost anomaly shows a westward dipping plate, which can be interpreted as a parallel antiform structure.

The modelled conductances were also in good agreement with those provided by Geotech Limited and the resistivity/conductivity measurements carried out on the massive sulphide samples from several Touro ore bodies. The combination of flat dips, good conductance, shallow depth, and the lack of conductive overburden or noneconomic conductive stratigraphy, such as graphitic shales and sulphide iron formations, made the Touro project an ideal target for airborne electromagnetic prospecting.

The 2017 VTEM airborne electromagnetic survey over the Touro project area proved very successful in mapping all the known Touro ore bodies, i.e., Monteminas, Bama, Arca, and Arinteiro, while also detecting several new targets with a high probability of being related to economic mineralisation, i.e., T-2, T-14, and T-15, and confirming the probable northward extension of the Monteminas ore body to depth.

Favourable factors contributing to the success of the survey were the high contrast in resistivity/conductivity between the massive sulphide Touro ore and the host amphibolite and paragneiss, and the minimal interference from "nuisance" conductors, such as graphitic shales.

The results obtained indicated that the Maxwell software was an adequate choice for EM modelling in the Touro area. The conceptual model with thin and thick sheets in the Maxwell software approximated the real conductance.

References

1. Pan, G.; Harris, D.P. *Information Synthesis for Mineral Exploration*; Oxford University Press: New York, NY, USA, 2000.
2. Carranza, E.J.M. Controls on mineral deposit ocurrence inferred from analysis of their spatial pattern and spatial association with geological features. *Ore Geol. Rev.* **2009**, *35*, 383–400. [CrossRef]
3. Hopgood, J.D.; Hungerford, N. Geophysical case history of the discovery of the Aguas Tenidas East Massive Sulphide Deposit, SW Spain. *Explor. Geophys.* **1994**, *25*, 1–17. [CrossRef]
4. Oliveira, V.; Matos, J.; Bengala, M.; Silva, N.; Sousa, P.; Torres, L. Geology and geophysics as successful tools in the discovery of the Lagoa Salgada Orebody (Sado Tertiary Basin-Iberian Pyrite Belt) Grandola, Portugal. *Miner. Depos.* **1998**, *33*, 170–187. [CrossRef]
5. McIntosh, S.M.; Gill, J.P.; Mountford, A.J. The geophysical response of the Las Cruces Massive Sulphide Deposit. *Explor. Geophys.* **1999**, *30*, 123–134. [CrossRef]
6. Guo-Qiang, X.; Ke-Zhang, Q.; Xiu, L.; Guang-Ming, L.; Zhi-Peng, Q.; Nan-Nan, Z. Discovery of a large-scale porphyry molybdenum deposit in Tibet through a modified TEM exploration method. *J. Environ. Eng. Geophys.* **2012**, *17*, 19–25.
7. Kowalczyk, P.; Bloomer, S.; Kowalczyk, M. Geophysical methods for the mapping of submarine massive sulphide deposits. In Proceedings of the Offshore Technology Conference, Houston, TX, USA, 4–7 May 2015.

8. Woolrych, T.R.H.; Christensen, A.N.; McGill, D.L.; Whiting, T. Geophysical methods used in the discovery of the Kitumba iron oxide copper gold deposit. *Interpretation* **2015**, *3*, SL15–SL25. [CrossRef]

9. Mostafaei, K.; Ramazi, H. Investigating the applicability of induced polarization method in ore modelling and drilling optimization: A case study from Abassabad, Iran. *Near Surf. Geophys.* **2019**, *17*, 637–652. [CrossRef]

10. Donoso, G.A.; Malehmir, A.; Pacheco, N.; Araujo, V.; Penney, M.; Carvalho, J.; Spicer, B.; Beach, S. Potential of legacy 2D seismic data for deep targeting and structural imaging at Neves-Corvo massive sulphide-bearing deposit, Portugal. *Geophys. Prospect.* **2020**, *68*, 44–61. [CrossRef]

11. Legault, J.M.; Plastow, G.; Zhao, S.; Bournas, N.; Prikhodko, A.; Orta, M. ZTEM and VTEM airborne EM and magnetic results over the Lalor copper-gold volcanogenic massive sulfide deposit region, near Snow Lake, Manitoba. *Interpretation* **2015**, *3*, SL83–SL94. [CrossRef]

12. Yang, D.; Fournier, D.; Kang, S.; Oldenburg, D.W. Deep mineral exploration using multi-scale electromagnetic geophysics: The Lalor massive sulphide deposits case study. *Can. J. Earth Sci.* **2019**, *56*, 544–555. [CrossRef]

13. Kuo, L.; Song, S.; Yeh, E.; Chen, H. Clay mineral anomalies in the fault zone of the Chelungpu Fault, Taiwan, and their implications. *Geophys. Res. Lett.* **2009**, *36*, L18306. [CrossRef]

14. Baranwal, V.C.; Ronning, J.S.; Gautneb, H.; Brönner, M. Integrated interpretation of airborne EM and magnetic data for graphite exploration from Vesterålen area in Northern Norway. In Proceedings of the 7th International Workshop on Airborne Electromagnetics, AEM Extended Abstracts, Kolding, Denmark, 17–20 June 2018.

15. Dindi, E.; Maneno, J.B.J. Geological and geophysical characteristics of massive sulphide deposits: A case study of the Lirhanda Massive sulphide deposit of Western Kenya. *J. Afr. Earth Sci.* **2016**, *120*, 89–101. [CrossRef]

16. Biondo-Ribeiro, V.; Mantovani, M.S. A multi-disciplinary characterization of Heath Steele Belt Deposits, Bathurst Mining Camp: A basis for identifying new targets for the exploration. *Near Surf. Geophys.* **2017**, *15*, 322–331. [CrossRef]

17. Badham, J.; Williams, P.J. Genetic and exploration models for sulfide ores in metaophiolites, Northwest Spain. *Econ. Geol.* **1981**, *76*, 2118–2127. [CrossRef]

18. Williams, P.J. The genesis and metamorphism of the Arinteiro-Bama Cu deposits, Santiago de Compostela, Northwestern Spain. *Econ. Geol.* **1983**, *78*, 1689–1700. [CrossRef]

19. Noble, A. On the mineral resources and reserves of the Touro Copper Project. Available online: https://atalayamining.com/wp-content/uploads/2020/01/NI-43-101-Technical-Report-for-Proyecto-Touro.pdf (accessed on 15 September 2022).

20. Julivert, M.; Martínez, F.J. The Structure and Evolution of the Hercynian Fold Belt in the Iberian Peninsula. In *The Anatomy of Mountain Ranges*; Princeton University Press: Princeton, NJ, USA, 1987; Chapter 6; pp. 65–105.

21. Arenas, R.; Díez-Fernández, R.; Sánchez-Martínez, S.; Gerdes, A.; Fernández-Suárez, J.; Albert, R. Two-satge collision: Exploring the birth of Pangea in the Variscan terranes. *Gondwana Res.* **2014**, *25*, 756–763. [CrossRef]

22. Arias, M.; Nuñez, P.; Arias, D.; Gumiel, P.; Castañón, C.; Fuertes-Blanco, J.; Martin-Izard, A. 3D geological model of the Touro Cu deposit, a World-Class Mafic-Siliciclastic VMS Deposit in the NW of the Iberian Peninsula. *Minerals* **2021**, *11*, 85. [CrossRef]

23. Rubio-Pascual, F.J.; Arenas, R.; Díaz-García, F.; Martínez-Catalán, J.R.; Abati, J. Contrasting high-pressure metabasites from the Santiago Unit (Ordenes Complex, Northwestern Iberian Massif, Spain). *Spec. Pap. Geol. Soc. Am.* **2002**, *364*, 105–124.

24. Castiñeiras, P. Origen y evolución tectonotermal de las unidades de O Pino y Cariño (Complejos Alóctonos de Galicia). *Ser. Nova Terra* **2005**, *28*, 1–289.

25. Julivert, M.; Fontboté, J.M.; Ribeiro, A.; Nabais Conde, L.E. Mapa Tectónico de la Península Ibérica y Baleares, E 1:1000000. In *Memoria Explicativa*; Instituto Geológico y Minero de España: Madrid, Spain, 1972; 113p.

26. Farias, P.; Gallastegui, G.; González Lodeiro, F.; Marquínez, J.; Martín Parra, L.M.; De Pablo Macía, J.G.; Rodríguez Fernández, L.R. Aportaciones al conocimiento de la litoestratigrafia y estructura de Galicia Central. *Mem. Fac. Ciências Univ. Porto* **1987**, *1*, 411–431.

27. Witherly, K.; Irvine, R.; Morrison, R.B. The Geotech VTEM Time Domain Electromagnetic System. In Proceedings of the 74TH Annual Meeting and International Exposition, ASEG Extended Abstracts 1–4, Nashville, TN, USA, 19–23 May 2019.

28. Wolfgram, P.; Golden, H. Airborne EM applied to sulphide nickel—Examples and analysis. *Explor. Geophys.* **2001**, *32*, 136–140. [CrossRef]